IFSCC 2025 full paper (IFSCC2025-481)

Investigation of Bioactive Substances in Different Rose Varieties and Molecular Docking and Validation with Anti-Aging Receptor Proteins

Jiayue Chen* [1.2], Hui Le[1], Bindi Cai[1], Yuankun Liu[2], Qiuhong Feng[1]

[1]Guangdong Thanmelin Biotechnology Co., Ltd, Guangdong, [2] Veminsyn Biotechnology Ltd., Hangzhou，China

Abstract

Roses (*Rosa spp.*) are rich sources of bioactive compounds with potential skincare applications, yet the relationship between cultivar-specific pigmentation, metabolite composition, and anti-aging efficacy remains unclear. This study integrated metabolomics and molecular docking to compare three rose cultivars—*Rosa hybrida* (Ser.) *Posp.* (black rose) , *Rose De Granville* (pink rose), and *Rose Pink Floyd* (purple rose)—focusing on their antioxidant profiles and mechanisms of anti-aging. UPLC-MS/MS identified 1,972, 1,819, and 1,777 metabolites in black, pink, and purple roses, respectively, with cyanidin-3,5-O-diglucoside as the dominant anthocyanin, showing a concentration gradient aligned with petal darkness (black rose > purple rose > pink rose). Flavonoids like tiliroside and phlorizin exhibited cultivar-specific accumulation. Molecular docking revealed strong binding of cyanidin-3,5-O-diglucoside to SIRT1, SIRT2, SIRT3 and SIRT6, while transcriptomics confirmed regulates photoaging-related signaling pathways in human keratinocytes cells with black rose extracts. These results establish that darker-pigmented roses possess superior anti-aging potential due to synergistic interactions between anthocyanins, flavonoids, and longevity pathways. This work provides a rationale for selecting pigment-specific roses in natural skincare development.

Keywords: *Rosa hybrida* (Ser.) *Posp.*; natural bioactive; skin anti-aging; metabolomics; molecular docking

1. Introduction

Roses (*Rosa spp.*), valued for their bioactive flavonoids, polyphenols, and anthocyanins, exhibit significant antioxidant and anti-aging properties, making them promising natural ingredients in skincare [1,3]. However, the metabolomic profiles and skincare-related bioactivities of *Rosa hybrida* (Ser.) *Posp.* (black rose), *Rose De Granville* (pink rose), and *Rose Pink Floyd* (purple rose)—three cultivars with distinct floral pigmentation—remain underexplored. Existing studies on these varieties focus primarily on horticultural traits [2], neglecting their phytochemical diversity, species-specific antioxidant capacity, and molecular mechanisms linked to skin aging. Notably, while anthocyanins (e.g., cyanidin-3,5-O-diglucoside) and flavonoids (e.g., tiliroside) are recognized as key antioxidants, their abundance in these cultivars and interactions with anti-aging targets (e.g., SIRTs, retinoic acid receptors) are poorly characterized. Furthermore, the correlation between petal coloration (a marker of anthocyanin content) and anti-aging efficacy remains unclear. This study integrates metabolomics, molecular docking and transcriptome to decode the cultivar-specific bioactive composition, validate ligand-receptor interactions, and elucidate regulatory effects on skin aging pathways, bridging critical gaps in leveraging these roses for advanced skincare applications.

2. Materials and Methods

Fresh petals of three rose cultivars, *Rosa hybrida* (Ser.) *Posp.* (black rose), *Rose De Granville* (pink rose), and *Rose Pink Floyd* (purple rose) were collected, freeze-dried, and extracted with 70% methanol for metabolite profiling. Metabolites were analyzed using UPLC-MS/MS (Exion LC^{TM} AD and Tandem mass spectrometry) with a Agilent SB-C18 column (1.8 μm, 2.1 × 100 mm), positive/negative ion modes, and a 0.35 mL/min flow rate. Raw data were processed with Multi Quant (v3.0.3) and matched against HMDB and KEGG databases. Anthocyanins and flavonoids were quantified by external standard curves (cyanidin-3,5-O-diglucoside, tiliroside, etc.), with triplicate biological replicates (N=3).For molecular docking, receptor proteins (SIRT1, PDB ID: 4IF6; SIRT2, PDB ID: 5D7O;SIRT 3, PDB ID: 4BN4; SIRT6, PDB ID: 3K35; RARA, PDB ID:5K13; RXRA PDB ID: 1RXR) were retrieved from PDB, optimized via AutoDockTools (v1.5.7), and docked with ligands (cyanidin-3,5-O-diglucoside, nicotiflorin, tiliroside, neochlorogenic acid, phlorizin, gallic acid) using AutoDock Vina (v1.2.0). To ensure the accuracy of the docking calculations, PyMOL was used to remove water molecules and irrelevant small-molecule ligands from the structures. Grid boxes covered binding pockets with 20 Å dimensions. Docking scores (kcal/mol) were averaged across 40 runs.

After 24 hours of treatment with either black rose extracts or DMEM medium (solvent control and UVB groups) HaCaTs were irradiated with UVB (60 J/cm^2), except for the solvent control group. Cells were then collected, and total RNA was extracted for RNA-seq analysis to evaluate the effects of black rose extracts on photoaging. High-throughput sequencing was conducted on an Illumina platform by NoVo gene Co., Ltd. (Beijing, China). Differential expression analysis was conducted between the model and black rose extracts-treated groups. Genes with an adjusted p-value < 0.05 were considered differentially expressed. Gene Ontology (GO)

and Kyoto Encyclopedia of Genes and Genomes (KEGG) enrichment analyses were performed to identify significantly enriched biological processes and pathways.

3. Results

3.1 Metabolite Profiling Reveals Species-Specific Active Component Diversity

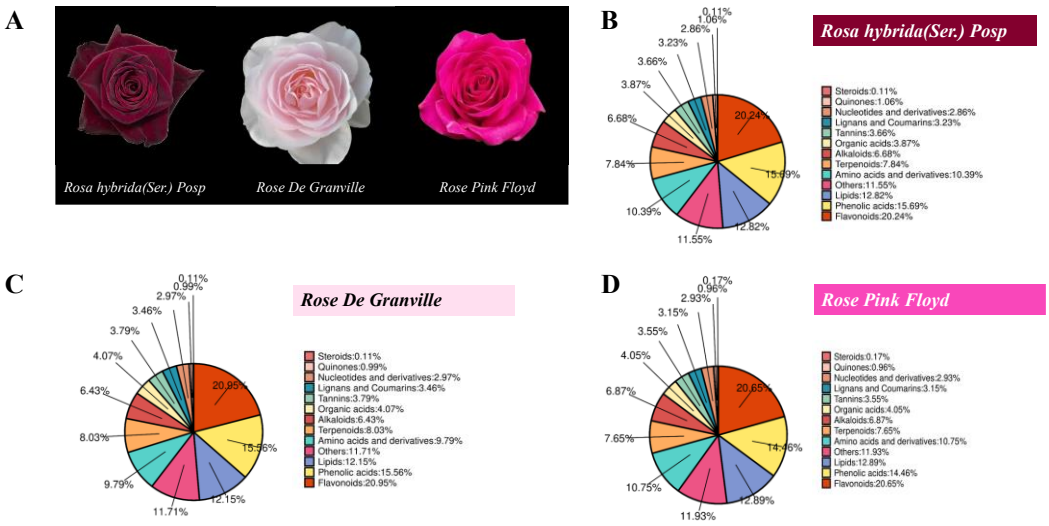

Figure 1. Qualitative analysis of active metabolites in three rose varieties with different petal colors using UPLC-MS/MS. (A) Phenotypic images of the three rose cultivars. (B) Distribution of 1,972 active metabolites identified in black roses (*Rosa hybrida* (Ser.) *Posp*). (C) Distribution of 1,819 active metabolites detected in pink roses (*Rose De Granville*). (D) Distribution of 1,777 active metabolites found in purple roses (*Rose Pink Floyd*). The samples were freeze-dried and extracted with 70% methanol for metabolite profiling. Qualitative analysis mainly included flavonoids, phenolic acid, lipids, amino acid and derivatives, terpenoids, alkaloids, organic acids, tannins, lignans and coumarins, quinones and steroids. N=3.

UPLC-MS/MS-based metabolomic analysis identified a total of 1,972, 1,819, and 1,777 active metabolites in black rose, pink rose, and purple rose, respectively (Figure 1B-D). The black rose exhibited the highest metabolic diversity. The secondary metabolites predominantly identified in three rose varieties were flavonoid and phenolic acid compounds (Figure 1B-D). Specifically, 709 compounds were detected in black roses, 664 in pink roses, and 623 in purple roses, suggesting that black rose may harbor a higher abundance of bioactive components. Notably, the anthocyanins that are related to the color of the petals belong to flavonoids. Phenotypic images (Figure 1A) highlighted distinct petal coloration, with darker pigmentation in the black rose correlating with elevated anthocyanin content. Therefore, further quantification of anthocyanins and flavonoids will be conducted to validate their functional properties.

3.2 Anthocyanin and Flavonoid Composition Exhibits Cultivar-Specific Patterns

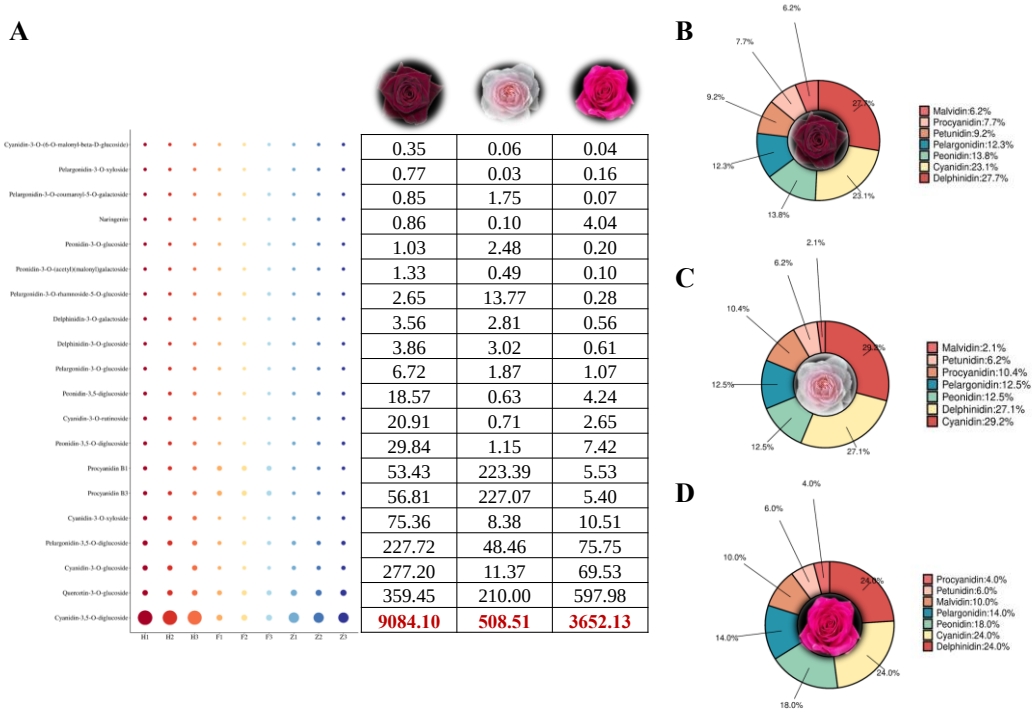

0.35	0.06	0.04
0.77	0.03	0.16
0.85	1.75	0.07
0.86	0.10	4.04
1.03	2.48	0.20
1.33	0.49	0.10
2.65	13.77	0.28
3.56	2.81	0.56
3.86	3.02	0.61
6.72	1.87	1.07
18.57	0.63	4.24
20.91	0.71	2.65
29.84	1.15	7.42
53.43	223.39	5.53
56.81	227.07	5.40
75.36	8.38	10.51
227.72	48.46	75.75
277.20	11.37	69.53
359.45	210.00	597.98
9084.10	**508.51**	**3652.13**

Figure 2. Quantitative analysis of anthocyanin contents and composition in three rose varieties with different petal colors using UPLC-MS/MS. (A) Variation trends of the top 20 most abundant anthocyanin composition across the three rose cultivars. H represents black rose (*Rosa hybrida* (Ser.) *Posp*); F represents pink rose (*Rose De Granville*); Z represents purple rose (*Rose Pink Floyd*). N=3. The greater dots, the higher anthocyanin contents. The value represents the contents of anthocyanin (ug/g, DW). Cyanidin-3,5-O-diglucoside content in black rose is 17.9 times higher than it in pink rose, and 2.5 times higher than it in purple rose. Distribution profile of anthocyanins in black roses (B), pink roses (C) and purple roses (D).

Analysis of anthocyanins (Figure 2B-D) revealed that cyanidin derivatives were the predominant components in the black rose, with significantly higher abundance compared to the purple and pink cultivars. Notably, cyanidin-3,5-O-diglucoside emerged as the most abundant anthocyanin across all cultivars, showing a concentration gradient aligned with petal color intensity: black rose (9084.1 μg/g) > purple rose (3652.13 μg/g) > pink rose (508.51 μg/g) (Figure 2A). Different classes of anthocyanidins exhibit inherent color variations. For example, the portion of malvidin (reddish-purple color) is found higher in black rose. It is in accordance with that black rose has deeper pigmentation.

Similarly, flavonoid analysis (Figure 3B-D) demonstrated significant interspecies variation. Tiliroside, a potent antioxidant flavonoid, was enriched in the black rose (173.13 μg/g), 19 times higher than both the pink and purple cultivar (Figure 3A). Nicotiflorin content in black

rose is 6.1 times higher than it in pink rose, and 5.0 times higher than it in purple rose (Figure 3A). Phlorizin content in black rose is 13.1 times higher than it in pink rose, and 2.5 times higher than it in purple rose (Figure 3A).

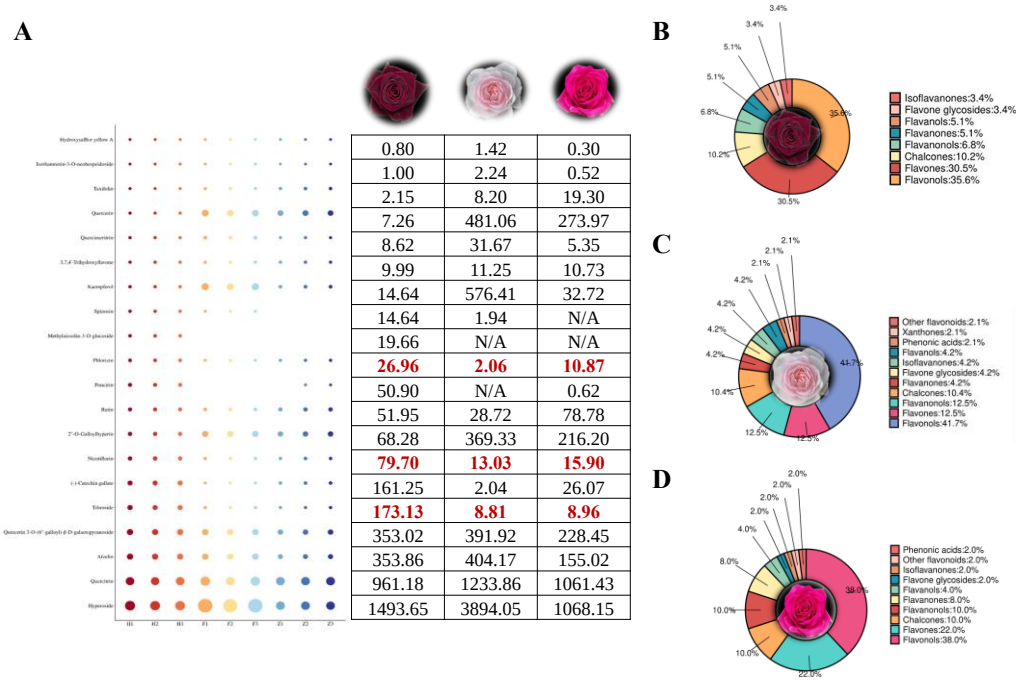

0.80	1.42	0.30
1.00	2.24	0.52
2.15	8.20	19.30
7.26	481.06	273.97
8.62	31.67	5.35
9.99	11.25	10.73
14.64	576.41	32.72
14.64	1.94	N/A
19.66	N/A	N/A
26.96	**2.06**	**10.87**
50.90	N/A	0.62
51.95	28.72	78.78
68.28	369.33	216.20
79.70	**13.03**	**15.90**
161.25	2.04	26.07
173.13	**8.81**	**8.96**
353.02	391.92	228.45
353.86	404.17	155.02
961.18	1233.86	1061.43
1493.65	3894.05	1068.15

Figure 3. Quantitative analysis of flavonoid contents and composition in three rose cultivars with distinct petal colors. (A) Variation trends of the top 20 most abundant flavonoids among the three rose varieties. The value represents the contents of flavonoid (μg/g, DW). H represents black rose (*Rosa hybrida* (Ser.) *Posp*); F represents pink rose (*Rose De Granville*); Z represents purple rose (*Rose Pink Floyd*). N=3. The greater dots, the higher anthocyanin contents. Tiliroside content in black rose is 19 times higher than it in pink rose and purple rose. Nicotiflorin content in black rose is 6.1 times higher than it in pink rose, and 5.0 times higher than it in purple rose. Phlorizin content in black rose is 13.1 times higher than it in pink rose, and 2.5 times higher than it in purple rose. Distribution profile of flavonoid in black roses (B), pink roses (C) and purple roses (D).

3.3 Molecular Docking Identifies Key Bioactives with High Anti-Aging Receptor Affinity

Molecular docking analysis (Table 1; Figure 4) evaluated four bioactive compounds (cyanidin-3,5-O-diglucoside, nicotiflorin, tiliroside, phlorizin), which were screened from quantitative analysis of anthocyanin and flavonoid, against SIRT1 [4] , SIRT2 [6] , SIRT3 [5] , SIRT6 [4] , RARA [7] , and RXRA [8] protein receptors. Neochlorogenic acid [10] and gallic acid [9] are the typical antioxidant bioactive in plants, they have been also detected in three rose varieties. They are also selected as a ligand in the following molecular docking experiment.

Cyanidin-3,5-O-diglucoside, as the characteristic component in black rose, exhibited the strongest binding to SIRT1 (forming hydrogen bonds with Gly-6, Gln-322, Pro-323 Leu-325,

and Lys-328 residues) , SIRT3 (forming hydrogen bonds with Thr-150, Gly-153 and Arg-345 residues) , SIRT2 (forming hydrogen bonds with Tyr-104, Asp-105, Glu-116 and Glu-288 residues) and SIRT6 (forming hydrogen bonds with Ala-51, Arg-63, Gln-111, Leu-184 and Trp-186 residues) , respectively (Figure 4A-D). Phlorizin showed high affinity for RXRA (forming hydrogen bonds with Ser-143, Lys-145, Tyr-147 and Glu-207 residues) (Figure 4F). Notably, the binding capacity between nicotiflorin and RARA (forming hydrogen bonds with Thr-261, Ser-390 and Leu-416 residues) was the highest (Figure 4E). Cyanidin-3,5-O-diglucoside displayed broad receptor interaction (Table 1). Neochlorogenic acid and gallic acid did not show good affinity in molecular docking experiments. These results suggest that cyanidin-3,5-O-diglucoside may serve as primary anti-aging agents in darker-pigmented roses.

Table 1. Docking Scores of Receptors with cyanidin-3,5-O-diglucoside, tiliroside, nicotiflorin, neochlorogenic acid, phlorizin and gallic acid.

Receptor	Ligand	Docking Score
SIRT1	Tiliroside	-7.71
	Nicotiflorin	-7.69
	Neochlorogenic acid	-7.43
	Phlorizin	-7.12
	Gallic acid	-4.64
	Cyanidin-3,5-o-diglucoside	**-7.75**
SIRT2	Tiliroside	-7.71
	Nicotiflorin	-7.96
	Neochlorogenic acid	-7.09
	Phlorizin	-7.49
	Gallic acid	-4.71
	Cyanidin-3,5-o-diglucoside	**-9.09**
SIRT3	Tiliroside	-7.22
	Nicotiflorin	-7.02
	Neochlorogenic acid	-5.37
	Phlorizin	-6.68
	Gallic acid	-4.17
	Cyanidin-3,5-o-diglucoside	**-8.03**
SIRT6	Tiliroside	-7.51
	Nicotiflorin	-7.91
	Neochlorogenic acid	-6.73
	Phlorizin	-8.17
	Gallic acid	-4.7
	Cyanidin-3,5-o-diglucoside	**-8.55**
RARA	Tiliroside	-6.25
	Nicotiflorin	**-8.57**
	Neochlorogenic acid	-6.46
	Phlorizin	-7.45
	Gallic acid	-3.94
	Cyanidin-3,5-o-diglucoside	-7.52
RXRA	Tiliroside	-5.72
	Nicotiflorin	-5.32
	Neochlorogenic acid	-6
	Phlorizin	**-7.28**
	Gallic acid	-4.4
	Cyanidin-3,5-o-diglucoside	-7.13

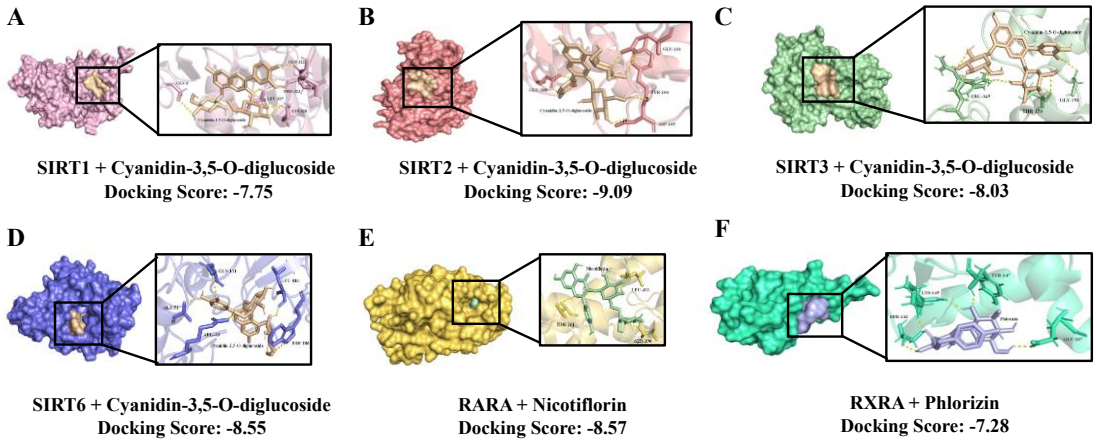

Figure 4. The molecular docking results of cyanidin-3,5-O-diglucoside, nicotiflorin and phloridzin with SIRT1, SIRT2, SIRT3, SIRT6, RARA and RXRA produced by PyMOL visualization software. Structural comparison of two molecular-protein interactions. Black boxes indicate binding interfaces, with zoomed-in views highlighting key interactions. Yellow dashed lines represented hydrogen bonds, distances were in angstroms. (A) SIRT1 protein is pink; (B) SIRT2 protein is red; (C) SIRT3 protein is green; (D) SIRT6 protein is purple; (E) RARA protein is yellow; (F) RXRA protein is turquoise.

3.4 RNA-seq was employed to establish the anti-aging biological activity of black rose extract.

RNA-seq was employed to explore the anti-photoaging mechanisms of black rose extract in cultured HaCaTs. The transcriptome profile of black rose extract-treated cells was compared with that of the UVB-treated group (60 J/cm²). Following treatment with black rose extract, a total of 342 differentially expressed genes (DEGs) were identified ($|Log_2FC|>1$, P-value<0.05), including 158 up-regulated and 184 down-regulated DEGs (Figure 5A). GO enrichment analysis and KEGG pathway analysis revealed that these DEGs were primarily implicated in response to UV, positive regulation of response to external stimulus, inflammatory response, and processes associated with dermatoses receptors (Figures 5B and 5C).

GO and KEGG pathway analysis demonstrated that the NF-κB signaling, HIF-1 signaling，TNF signaling, Toll-like receptor and Nod-like receptor signaling pathways were significantly enriched. Specifically, the expression of six inflammation-associated genes (including *SAA1, SAA2, CXCR2, CCL2, CCHCR1*, and *ATF6B*) and six oxidative stress and homeostasis related genes (including *VARS2, UBE2A, NMRAL1, MCRIP1, FBXO42* and *TEP1*) was significantly improved by black rose extract, in response to UV stress (Table 2; P <0.05). Collectively, these findings suggest that black rose extracts may combat skin photoaging by modulating skin inflammation, enhancing oxidative stress resistance, and improving cellular homeostasis.

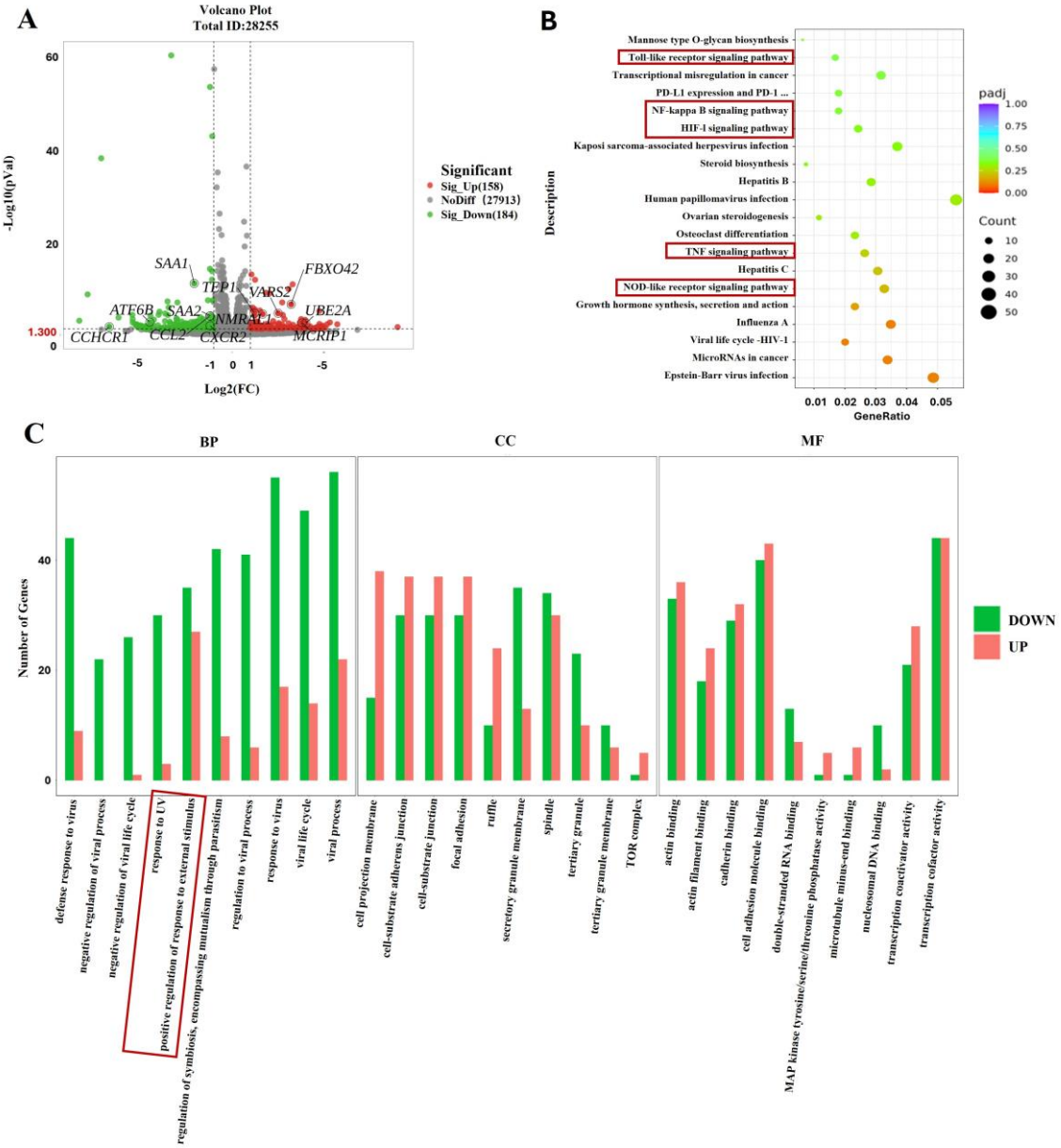

Figure 5. Identification of DEGs and enrichment analysis. Data are presented as mean±SD (n = 3). (A) Volcano plot of DEGs: upregulated genes are shown in red and down regulated genes in green (p-value< 0.05, |Log2FC|⩾1). (B) Top 20 enriched KEGG pathways, Dot size and color indicate the number of enriched DEGs and statistical significance, respectively. (C) Top 10 enriched GO terms in BP (Biological Process), CC (Cellular Component), and MF (Molecular Function) categories, ranked by adjusted p-value. Gene Ratio represents the proportion of enriched DEGs to total DEGs. Column height and color indicate the number of enriched DEGs and the expression trend, respectively.

Table 2. Twelve representative DEGs differentially expressed by black roses extracts treatment. Log2FC represents the log base 2-fold change, which is used to quantify the magnitude of gene expression differences between two groups of samples. P-value (Probability value) is a statistical measure used to assess the significance of a result obtained in a hypothesis test.

Gene Name	NCBI ID	Description	Log_2FC	P-value
VARS2	NM_001167733.3	Valyl-trna synthetase 2	2.506048696	2.24×10^{-5}
UBE2A	NM_001282161.2	Ubiquitin conjugating enzyme e2 a	4.019305864	0.00297770
TEP1	NM_001319035.2	Telomerase associated protein 1	1.2133451	2.11×10^{-5}
SAA2	NM_001127380.3	Serum amyloid a1	-1.177073	8.33×10^{-5}
SAA1	NM_000331.6	Serum amyloid a2	-2.057297	9.45×10^{-12}
NMRAL1	NM_001305141.3	Nmra like redox sensor 1	1.6664502	3.34×10^{-5}
MCRIP1	NM_001093767.3	Mapk regulated corepressor interacting protein 1	3.8037289	0.0025165
FBXO42	NM_018994.3	F-box protein 42	3.2093474	2.82×10^{-7}
CXCR2	NM_001168298.2	C-x-c motif chemokine receptor 2	-1.190873	0.0103271
CCL2	NM_002982.4	C-c motif chemokine ligand 2	-1.21294	9.91×10^{-5}
CCHCR1	NM_001105563.3	Coiled-coil alpha-helical rod protein 1	-6.673948	0.0178695
ATF6B	NM_001136153.2	Activating transcription factor 6 beta	-4.47715	0.0017829

4. Discussion

This study establishes a direct link between rose petal coloration and anti-aging bioactivity, with darker-pigmented cultivars (*Rosa hybrida (Ser.) Posp.*) exhibiting superior antioxidant/anti-aging potential due to cyanidin-3,5-O-diglucoside dominance. The high affinity of cyanidin derivatives for SIRTs and retinoid receptors aligns.

The ultraviolet (UV)-induced inflammation and subsequent ROS accumulation are central effectors in photoaging [11]. UV exposure triggers inflammation by releasing pro-inflammatory cytokines (e.g., *IL-1, IL-6*) from the stratum corneum and stimulating TNF-α synthesis and release from keratinocytes. These key cytokines then induce the synthesis and release of other pro-inflammatory cytokines in response to UV exposure. As the main organ directly exposed to UV radiation, the skin is commonly affected by UV-induced oxidative stress, which causes DNA damage. Post-UV exposure, the antioxidant system balance is disrupted, inducing oxidative stress and affecting deep skin structures. Accumulated oxidative stress damages skin cellular components, leading to photodamage and photoaging [11]. RNA-seqs studies have demonstrated that black rose extract plays a role in slowing down skin aging. In this study, black rose extract modulated multiple inflammation-related signaling pathways, including the NF-κB, TNF and Toll-like receptor signaling pathways (Figure 5). As shown in Figure 5, after UV exposure, black rose extract also participates in cellular oxidative stress processes by regulating the HIF-1 pathway. Black rose extract combats photoaging mainly through relieving inflammation and oxidative stress, which is in line with the antioxidant and anti-inflammatory properties of anthocyanins. These findings advance the selection of pigment-specific roses for tailored skincare formulations, although vivo validation remains essential.

5. Conclusion

This study systematically characterized the metabolomic profiles of three rose cultivars and identified cyanidin-3,5-O-diglucoside, nicotiflorin and phlorizin as key bioactive compounds with significant anti-aging potential. The black rose (*Rosa hybrida*) demonstrated superior antioxidant capacity due to its unique anthocyanin and flavonoid composition. These findings provide valuable insights for developing rose-based anti-aging products and establish a foundation for further research on plant-derived cosmetic ingredients.

6. Acknowledgments

NONE.

7. Conflict of Interest Statement

NONE.

8. Reference

[1]. Cendrowski, A., Ścibisz, I., Mitek, M., Kieliszek, M., & Kolniak-Ostek, J. (2017). Profile of the phenolic compounds of Rosa rugosa petals. *Journal of food quality*, *2017*(1), 7941347.
[2]. Debener, T., & Linde, M. (2009). Exploring complex ornamental genomes: the rose as a model plant. Critical reviews in plant sciences, 28(4), 267-280.
[3]. Hoang, H. T., Moon, J. Y., & Lee, Y. C. (2021). Natural antioxidants from plant extracts in skincare cosmetics: Recent applications, challenges and perspectives. *Cosmetics*, *8*(4), 106.
[4]. You Y, Liang W. (2023). SIRT1 and SIRT6: The role in aging-related diseases. *Biochimica et biophysica acta. Molecular basis of disease.* 2023(7):166815.
[5]. McDonnell, E., Peterson, B. S., Bomze, H. M., & Hirschey, M. D. (2015). SIRT3 regulates progression and development of diseases of aging. *Trends in endocrinology and metabolism.* 26(9), 486–492.
[6]. Kaitsuka, T., Matsushita, M., & Matsushita, N. (2021). Regulation of Hypoxic Signaling and Oxidative Stress via the MicroRNA-SIRT2 Axis and Its Relationship with Aging-Related Diseases. *Cells*, *10*(12), 3316.
[7]. Watson, R. E., Arjuna Ratnayaka, J., Brooke, R. C., Yee-Sit-Yu, S., Ancian, P., & Griffiths, C. E. (2004). Retinoic acid receptor alpha expression and cutaneous ageing. *Mechanisms of ageing and development*, 125(7), 465–473.
[8]. Martin, N., Ma, X., & Bernard, D. (2019). Regulation of cellular senescence by retinoid X receptors and their partners. *Mechanisms of ageing and development,* 183, 111131.
[9]. Shan, H., Geng, L., Jiang, X., Song, M., Wang, J., Liu, Z., Zhuo, X., Wu, Z., Hu, J., Ji, Z., Wang, S., Chan, P., Qu, J., Zhang, W., & Liu, G. H. (2022). Large-scale chemical screen identifies Gallic acid as a Gero protector for human stem cells. *Protein & cell*, 13(7), 532–539.
[10]. Ahn, H. S., Kim, H. J., Na, C., Jang, D. S., Shin, Y. K., & Lee, S. H. (2021). The Protective Effect of Adenocaulon himalaicum Edgew. and Its Bioactive Compound Neochlorogenic Acid against UVB-Induced Skin Damage in Human Dermal Fibroblasts and Epidermal Keratinocytes. *Plants (Basel, Switzerland)*, 10(8), 1669.
[11]. Pillai, S., Oresajo, C., & Hayward, J. (2005). Ultraviolet radiation and skin aging: roles of reactive oxygen species, inflammation and protease activation, and strategies for prevention of inflammation-induced matrix degradation-a review. *International journal of cosmetic science*, 27(1), 17–34.